Original Article

Andreas Himmelsbach, Tobias Standau, Johannes Meuchelböck, Volker Altstädt and Holger Ruckdäschel*

Approach to quantify the resistance of polymeric foams against thermal load under compression

https://doi.org/10.1515/polyeng-2021-0312
Received October 29, 2021; accepted December 2, 2021; published online February 10, 2022

Abstract: Nowadays, numerous techniques are used to quantify the resistance of cellular polymers against a thermal load. These techniques differ in significance and reproducibility and are all dependent on foam density, structure (i.e., cell size and -distribution) and sample geometry. Very different behaviors are expected for extrusion- and bead foams, as well as for amorphous and semi-crystalline polymers. Moreover, established tests use temperature ramps which would lead to temperature gradients within the sample and thus to faulty results. In this study, we developed a new approach from an engineering perspective to minimize these influences. In this approach, the resistance against the thermal load is derived from a steady creep test with defined temperature steps under a mechanical load, which is specifically set for each foam sample depending on its static compression behavior at room temperature. The two-stage test therefore combines (i) a standard quasi-static compression test at room temperature and (ii) a creep test with stepwise increased thermal loading. For each foam type, a rather low mechanical load (stress) is determined from the quasi-static compression test at room temperature; low enough to remain below the collapse strength and avoid irreversible deformation (i.e., buckling and/or breaking of the cell walls). This load is then applied in a creep test where the temperature is increased in defined steps from room temperature to a temperature close to T_g or T_m. The stepwise increase and holding of the temperature for a defined time enables a homogeneous temperature in the test specimen. The approach was applied to (i) polystyrene extrusion and bead foams (i.e., XPS and EPS), which have different foam structure, (ii) amorphous and semi-crystalline bead foams of polystyrene (EPS) and polypropylene (EPP), (iii) bead foams with different densities (30, 60, 120, and 210 kg/m^3) and (iv) to a new type of bead foam made of the engineering polymer polybutylene terephthalate (E-PBT). The termination criterion for the test is defined as the temperature at which a relative compression of 10% is reached in the creep test with temperature steps. We suggest calling it the heat stability temperature T_{HS}. For the studied foams, the procedure delivers characteristic T_{HS} values that allow a good comparison between different polymer matrices and densities. The heat stability temperature T_{HS} of amorphous PS foams (i.e., XPS and EPS) was determined to be 98 °C, which is close to the glass transition temperature T_g. Using the same approach, values of 99–107 °C were determined for EPP and 186 °C for the semi-crystalline bead foam E-PBT.

Keywords: compression test; foams; heat stability temperature; mechanical testing; steady creep test.

1 Introduction

The mechanical behavior of foams was well described in fundamental studies by Ashby [1, 2], stating that the typical compression curve consists of three areas. This includes (i) a linear-elastic region at the beginning, where the deformation of the foam is reversible as the cell struts and walls elastically bend, followed by (ii) a plateau, where they get plasticly deformed (i.e., irreversible) by buckling and breakage, and (iii) finally a steep increase of stress, which is called densification, where the compressed foams start to behave like a compact material [3, 4]. The so called

Andreas Himmelsbach and Tobias Standau contributed equally to this work.

***Corresponding author: Holger Ruckdäschel,** Department of Polymer Engineering, University of Bayreuth, Universitätsstr. 30, 95447 Bayreuth, Germany, E-mail: holger.ruckdaeschel@uni-bayreuth.de
Andreas Himmelsbach, Tobias Standau and Johannes Meuchelböck, Department of Polymer Engineering, University of Bayreuth, Universitätsstr. 30, 95447 Bayreuth, Germany
Volker Altstädt, Department of Polymer Engineering, University of Bayreuth, Universitätsstr. 30, 95447 Bayreuth, Germany; and Bavarian Polymer Institute and Bayreuth Institute of Macromolecular Research, University of Bayreuth, Universitätsstr. 30, 95447 Bayreuth, Germany

collapse stress is located at the transition of linear-elastic region and the plateau. The compression behavior is primarily driven by the foams density and structure (e.g., thickness/length ratio of the cell walls). Usually, with increasing density, the struts become thicker and thereby more resistant against deformation (i.e., buckling). Also the cell gas influences the deformation behavior as it provides a certain counter pressure – a remarkable effect for closed-celled foams [5]. Generally, the compression behavior of foams differs with the density and a lower foam density would result in lower energy absorption as stated by Wei et al. [6]. Moreover, the compression strength is also influenced by the foam structure. In the works of Ramsteiner et al. [7] and Lim et al. [8] it was clearly shown that for cellular materials the compressive deformation is not homogeneously distributed over the whole foam bulk but stress bands appear in which the deformation accumulates while other regions stay unaffected.

Generally, with extrusion foams and bead foams similar densities and cell sizes are possible [9]. However, bead foams show a lower mechanical performance than extrusion foams at the same density [10]. This could be explained, as the extrusion foams – even though they have some inhomogeneities (i.e., mainly depending on the extrusion direction [11]) – are more uniform, while the bead foams could contain broad cell size distributions and/or voids in between the fused beads, that can be considered as defects. Also, it is known that during processing (i.e., extrusion) shear and die swell effects could lead to strong cell anisotropy [12, 13]. Anyhow, the mechanical behavior of bead foams is very complex [14] due to the existence of structural differences that are described by Coquard et al. [15] as macro- and micro-porosity. Interestingly, it could be seen from the works of Ossa et al. [16], that the macroporosity (e.g., voids between the beads) and at the microscopic level larger cells in the individual beads initiate the failure during compression as they are the weakest points.

In one of our previous studies [17] we have shown that smaller and homogeneously distributed cells are beneficial to distribute the applied load more evenly in the volume resulting in higher compression strength for PLA extrusion foams, even at a lower density. For polypropylene bead foams, similar findings were described by Bouix et al. [4]. Here, a linear correlation between density and compression strength was found within the investigated density range of 34–76 kg/m^3. Smaller cells are beneficial to achieve a higher collapse stress, as the cells tend less to buckle (irreversible, plastic deformation). The correlation between density and compression behavior was also confirmed by Castiglioni et al. [18] and Di Landro et al. [19].

One current trend is the development of bead foams with increased resistance against heat exposure and several attempts with mostly engineering polymers were made, such as PA 12 [20], PET [21] and PBT [22]. Surprisingly, no unified methods are used to quantify the resilience against heat of these materials. It is worth noting, that in this context several expressions can be found; e.g., "heat deflection/distortion temperature (HDT)" or "heat resistance" are most commonly used for the description of the thermo-mechanical behavior of materials. Standards, such as DIN EN ISO 75 [23] (to determine the HDT) or DIN EN ISO 306 [24] (so called Vicat Test) are designed for compact materials and are actually not suitable for cellular materials because of the required small sample sizes and the rather small area where the external load is applied. To our best knowledge, the only standard which was designed for foams – DIN 53424 – was meanwhile withdrawn. The principle of DIN 53424 [25] is to apply a constant load (10 g) either in a two-point bending or compression test while heating the sample continuously (at 50 K/h) and to measure a certain sample deformation (i.e., 10 mm deflection or 10% relative compression, respectively).

Non-standardized alternatives exist and were applied in scientific works and patents. It is possible to carry out compression tests at elevated but constant temperatures. This was done for EPS [26, 27], EPP [28, 29], and E-PBT [30]. Clearly, the strength decreases with increasing temperature. Also, in some works [20, 22] DMA measurements were applied to foams to make a statement about their resistance against elevating temperatures – typically under a temperature ramp and a very low mechanical load. A very early work of Takemori [31] explains typical DMA curves of amorphous and semi-crystalline polymers and summarizes the crystallinity, morphology, thermal history, molecular weight (distribution) as the key factors that govern the behavior of polymers under thermal load. Other tests, mainly applied by industry, are based on annealing the sample for several hours at a certain elevated temperature and judge the dimensional stability [32, 33].

It should be emphasized, that a non-neglectable temperature deviation between foam core and the test chamber can be expected when a temperature ramp like in the above mentioned standards [23–25] is applied, as the foams act as insulating materials. An effect that gets even more pronounced at low densities.

All these methods have limitations as foams with different densities and/or cell structures cannot be compared very well due to two overlapping effects; (i) the deformation driven by the applied mechanical load which is – as described before – strongly dependent on the density and the structure of the foam and (ii) the actual

deformation caused by the thermal load, which is assumed to be influenced by different material parameters such as T_g, T_m, crystallinity and thermal conductivity, respectively.

This work describes an approach from the engineering view to be able to quantify the resistance against thermal deformation aiming to allow the comparison of different foamed samples. For this purpose, steady creep tests with stepwise increased temperature and a low mechanical load that has a correlation with the individual foam were carried out. The approach was applied on amorphous and semi-crystalline polymeric foams, respectively. Furthermore, extrusion- and bead foams with different densities were investigated to evaluate whether the structural influences (e.g., foam density and morphology) on the determination of T_{HS} could be minimized.

2 Materials and methods

2.1 Materials

Different commercial extrusion- and bead foams made of polystyrene and polypropylene as well as novel noncommercialized bead foam made from PBT were used in this study. The materials and their densities are summarized in Table 1. The commercial expanded beads were fused to plates at Neue Materialien Bayreuth GmbH in the mould of a steam chest moulding machine (Teubert TVZ 125/85, Blumberg, Germany) according to the data sheets of the suppliers. Details for the preparation, processing and properties of the E-PBT and further information about the necessity of using chain extender can be found in our previous publications [22, 30, 34].

The extrusion foam (XPS) was purchased as a typical semi-finished product in board form without any outer skin. Cuboid specimens were cut out by an electric band saw exhibiting a ground area of $A = 40 \times 40$ mm^2 and an initial height $H_0 = 20$ mm. The EPS specimen was treated at 80 °C for 4 h in an oven to remove any residual blowing agent. All samples were conditioned for 3 days at 23 ± 2 °C and 50 ± 5% r.H. prior to testing. The sample names in this study are a combination of the materials designation and the density value. For example, the polystyrene extrusion foam with a density of 30 kg/m^3 is encoded with XPS_30.

Table 1: Summary of the used materials.

Material (designation)	Trade name (supplier)	Density (kg/m^3)
Extruded polystyrene (XPS)	Isopor-XPS (Isopor GmbH, Neunkirchen, Germany)	30
Expandable polystyrene (EPS)	A245 SE (Sunpor Kunststoff GmbH, St. Pölten, Austria)	30, 60
Expanded polypropylene (EPP)	Neopolen® P8015 (BASF SE, Ludwigshafen, Germany	30
	Neopolen® P9035 (BASF SE, Ludwigshafen, Germany)	60
	Neopolen® P9280 (BASF SE, Ludwigshafen, Germany)	120, 210
Expanded polybutylene terephthalate (E-PBT)	PBT Pocan® B1300 (Lanxess AG, Köln, Germany) +1 wt% Joncryl® (BASF SE, Ludwigshafen, Germany)	220

2.2 Methods

2.2.1 Foam morphology and density: For examining the foam morphology scanning electron microscopy (SEM) measurements were carried out on gold-sputtered samples with a scanning electron microscope (JEOL JSM-6510, Akishima, Japan) at an acceleration voltage of 10 kV. Cell sizes were then determined by use of an image analysis software (ImageJ, v1.48) considering at least 50 cells per image.

The density was determined for each specimen by the ratio of its dimension and weight.

2.2.2 Thermal analysis: To measure the thermal characteristics, a differential scanning calorimeter (DSC 1, Mettler Toledo (Columbus/OH, USA) was used. The measurements were carried out under nitrogen atmosphere in a temperature range of 25–150 °C (PS), −25 to 200 °C (PP) or 25–250 °C (PBT) at a heating rate of 10 K/min. The crystallinity was calculated from the melting enthalpy for a 100% crystalline PP, $\Delta H_{m,PP}$ = 207 J/g [35] or 100% crystalline PBT $\Delta H_{m,PBT}$ = 140 J/g [36], respectively.

2.2.3 Oven pretrials to determine the thermal inertia of foams: To analyze the temperature difference and -delay of the foams, some specimens were equipped with thermo-couples attached to a digital datalogger (PCE-T 390, PCE Instruments, Meschede, Germany) and put in a vacuum oven (Memmert VO, Büchenbach, Germany) at ambient pressure.

First, the temperature was increased up to 100 °C with a heating ramp of 50 K/h. Second, after reaching 100 °C the temperature was kept constant for 60 min. The temperatures of the oven and the foam cores of samples with different densities were monitored every 30 s and compared.

2.2.4 Mechanical testing: Static compression testing was performed according to DIN EN ISO 844 with a universal testing machine (Z050, Zwick & Roell GmbH & Co. KG, Ulm, Germany) equipped with a 50 kN load cell. A pre-force of 5 N was applied to the specimens (40 × 40 × 20 mm) which were then compressed to 50% H_0 with a constant test speed (10% H_0/min). To obtain a comparable compressive stress at 10% compression, the graph was adjusted with respect to run-in effects (triggered by the application of the pre-force). For this purpose, the graphs were shifted along the x-axis until the slope line of the elastic modulus intersects the zero point. For each material a series of three specimens was measured at 23 ± 2 °C and 50 ± 5% r.H. The deformation was determined by the traverse path.

Furthermore, the steady creep test with temperature steps was performed with a servo-hydraulic test machine (Instron GmbH, Darmstadt, Germany) equipped with an integrated heating chamber as well as a 10 kN load cell. The tests were done with cuboid specimens (40 × 40 × 20 mm) and the deformation was determined by the traverse path.

2.2.5 Approach to determine the heat stability temperature of foams: The approach used in this work to determine the heat stability temperature T_{HS} of foams are based on two steps, as schematically shown in Figure 1. The first step is a quasi-static compression test at room temperature according to DIN EN ISO 844 which is needed to define the later required comparably low mechanical load (similar to DIN 53424) adapting individually to the tested foam. Therefore, a tenth of the stress at 10% strain $\sigma_{10\%}$ in the compression curve – is calculated. This was denoted as $\sigma_{(10/10)\%}$. It was refused to directly use the measured stress at 1% relative compression due to possibly occurring fluctuation in the curves that are caused by running-in effects at the beginning of the measurements. The low load defined in this manner aims to stay underneath the collapse stress, to avoid irreversible deformation of the foam.

In the second step, a steady creep test with temperature steps is carried out with the before determined mechanical load $\sigma_{(10/10)\%}$. Prior to testing, specimens were preloaded (i.e., compression of 5 N) and compressed at a constant speed of 2 mm/min at constant temperatures until the previously determined force has been reached. It was necessary to do certain pretrials to set the step width and height for the temperature steps. During the actual test the temperature was increased in intervals of 10 K with a holding time of 5 min for each temperature step, while the compression was recorded continuously until the test criterion is reached. Here, the temperature regime was selected to ensure an equilibrium in the sample. It can be anticipated that with increasing test temperature the applied stress $\sigma_{(10/10)\%}$ will come closer to the collapse stress (which decreases with increasing test temperature [30]) and may even exceed it.

Three measurements were carried out for each material. The mean values of the relative compression were plotted against the foam core temperature.

Based on the older standard DIN 53424 (compression mode) [25], we defined the temperature at which the sample reaches 10% relative compression strain as the test criterion. However, a higher and lower relative compression strain was also considered and evaluated as test criteria.

The core temperature of the foams was measured and verified with the above-mentioned digital thermocouple with integrated datalogger.

The temperature range for testing was set depending on the thermal properties of the respective polymer. For XPS and EPS, this range was between +60 up to +100 °C, for EPP between +60 up to +120 °C and for E-PBT between +100 up to +200 °C.

3 Results and discussion

3.1 Preliminary tests and analysis

Several preliminary tests were carried out to quantify the thermal inertia of the foamed samples and to determine the thermal expansion of the compression tool set-up. Based on the knowledge gained, the height of the heating steps and the time periods required to reach the thermal equilibrium of the test set-up were determined.

Foams are used as insulation materials due to their low thermal conductivity. The thermal insulation properties depend, among other parameters, on their relative density, the cell size and the thermal conductivity of the polymer

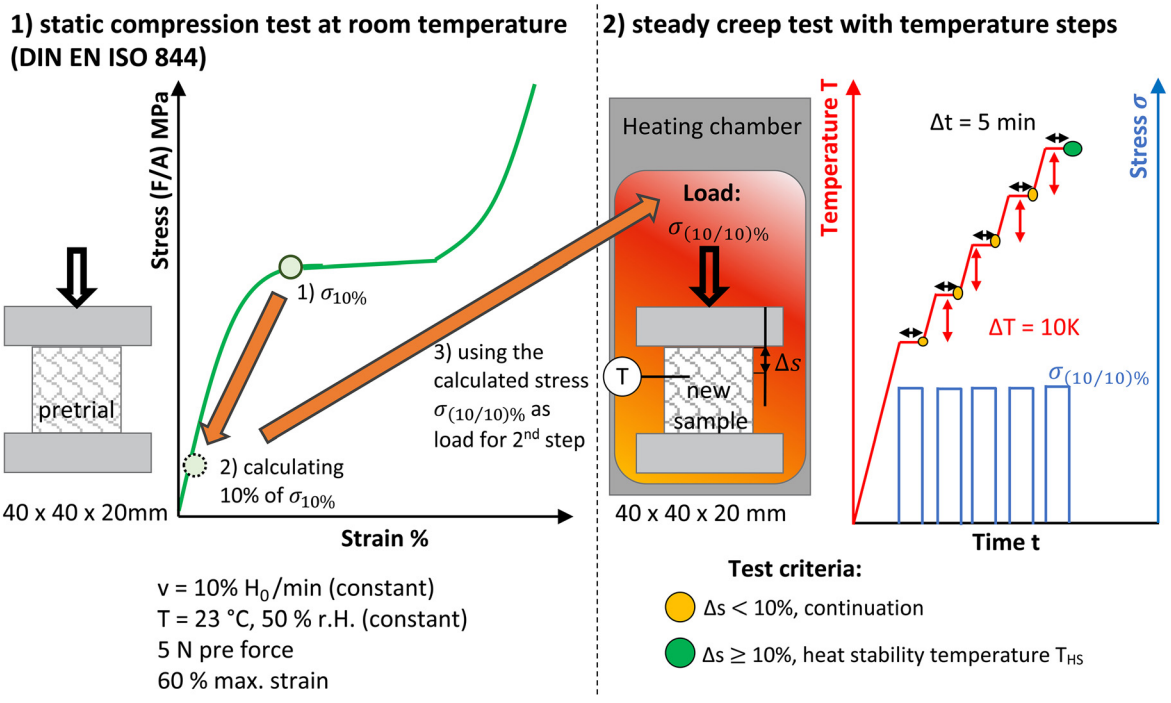

Figure 1: Concept of the approach: a static compression test is used in the 1st step to determine the test load $\sigma_{(10/10)\%}$ which is applied in a steady creep test with stepwise increased temperature in the 2nd step.

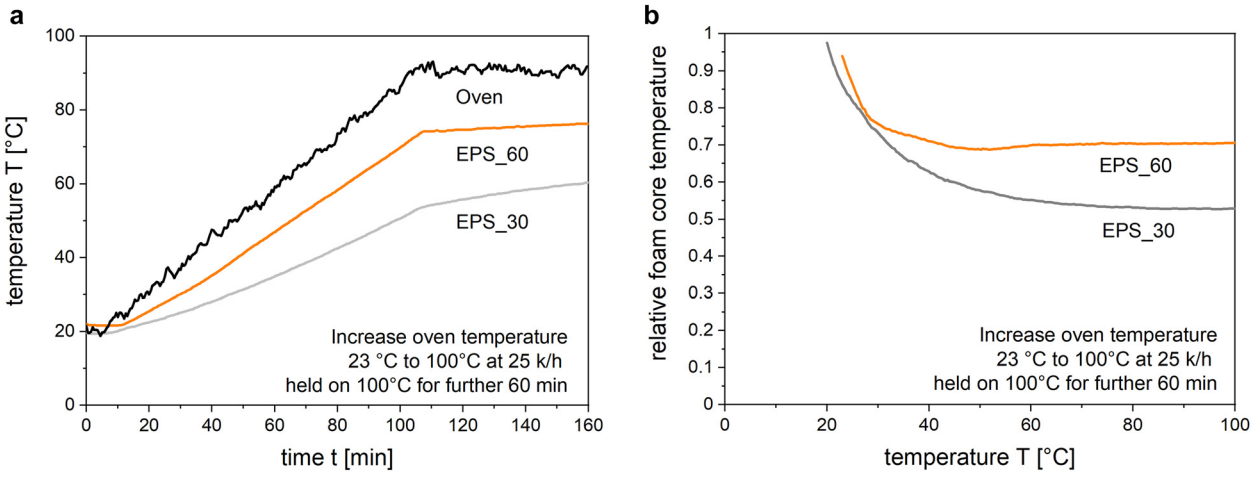

Figure 2: (a) Temperature of the oven and the cores of the samples EPS_30 and EPS 60. (b) Relative temperatures of the foam cores compared with the oven.

itself [37, 38]. Reaching the ambient temperature in the foam bulk is usually recorded with a time delay due to the thermal inertia; and in some cases an equilibrium cannot be reached at all in a reasonable time. In order to measure the thermal inertia, the heating rate was set to 50 K/min (0.8 K/min) in accordance to DIN 53424. However, the actual heating rate measured was lower (approx. 25 K/h). Anyhow, the time dependency of the oven temperature and the core of the samples of EPS_30 and EPS_60 are drawn in Figure 2a.

Depending on their density, the cores of the foams have a significant temperature difference compared to the ambient temperature in the oven. From Figure 2b it can be seen that the foam core temperatures deviates, meaning that EPS_30 reaches about 50% and EPS_60 about 70% of the ambient temperature. The curve of the relative temperature difference shows that the heat transfer decreases significantly as a function of the foam density.

This is due to the fact that lower densities usually result in lower thermal conductivity [39]. For example, at an oven temperature of 80 °C, the foam core temperature of EPS_30 is 47 °C and of EPS_60 is 47 °C. This means, the actual foam core temperature thus deviates by 15 K or 33 K from the measured oven temperature.

Taken these results into account, it can be assumed that the temperature that is supposed to quantify the resistance against thermal deformation measured according to DIN 53424 (or any other method where such a heat ramp is applied) does not correspond to the foam core temperature and the obtained values are flawed and not trustworthy.

In order to counteract the delayed rise in the foam temperature, the ambient temperature should be not increased continuously but gradually by 10 K steps with holding time giving the foam bulk sufficient time to adapt to the ambient temperature.

In further preliminary tests, the thermal expansion of the compression tool was investigated as a function of the oven temperature and the heating steps. A necessary equilibration time (i.e., no further thermal expansion of measuring system) of 20–40 min between 60 and 200 °C could be determined. The measurement of the foam core temperature during this conditioning shows that the thermal expansion of the measuring system (plates and pistons) is the time-limiting factor. The optimal measurement duration for each step of the steady creep tests was found to be 5 min. In this manner, the duration of the measurement in relation to the deviation of the averaged values in the equilibrium state is perceived as good.

Foam density was the main criteria for the sample selection. However, the corresponding structures (cell size and cell size distribution) are rather different. Representative SEM images of all samples are shown in Figure 3. It becomes evident, that not only the densities but also the cell sizes of the investigated foams cover a wide range.

3.2 Application of the approach

3.2.1 Step 1: static compression tests according to DIN EN ISO 844

As described above, the first step of the chosen approach is to perform a static compression test. The stress-strain curves for all samples are shown in Figure 4a and 4b. It can be clearly seen that the compression behavior of extrusion-

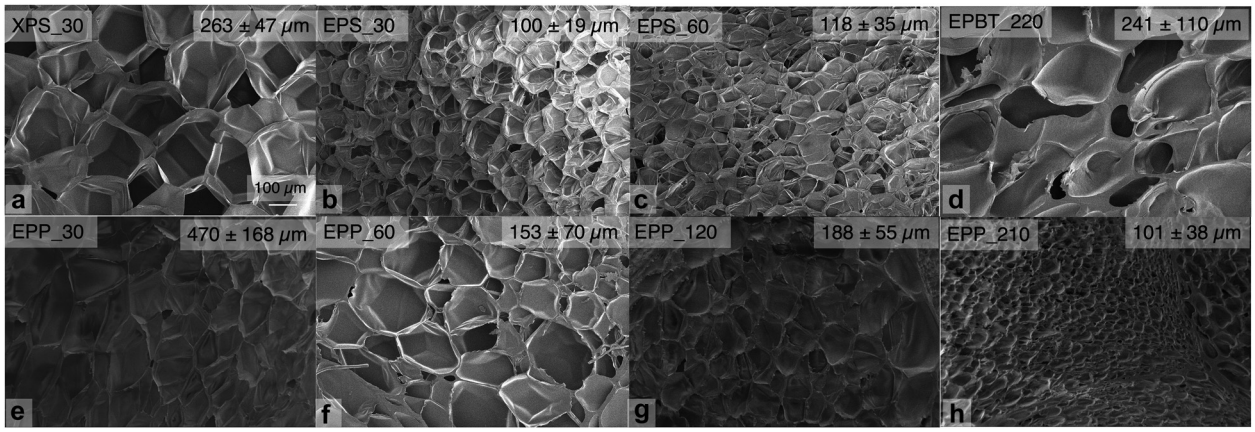

Figure 3: SEM images of the cellular morphology of the investigated foam samples.

and bead foams differs. XPS_30 shows a significantly higher stress plateau than the investigated bead foams with similar and even higher densities of 30 and 60 kg/m^3, respectively (cf. Figure 4a). The curves also reveal that, the modulus of elasticity of the bead foams and the collapse stress increase with foam density. As already shown by Wei et al. [6] the level of the stress plateau remains constant over a larger strain range, the lower the foam density is. Bouix et al. [4] found that the load up to the buckling of the cell walls increases with increasing density and finer cell structure. Furthermore, in closed-cell foams, the gas in the cells is compressed, which leads to an increase in stress as it is clearly visible for all of the investigated bead foams. The general behavior of the foamed samples agrees with the literature [3, 4, 6] for cellular materials.

The measured stress at 10% compression of XPS_30 is 0.48 MPa and is thereby almost three times higher than the stress of EPS_30 with 0.19 MPa. An increase in the foam density by a factor of 2 leads to a two-fold increase in the compression stress to 0.39 MPa for EPS_60. The results of the compression tests show that the foaming process and the resulting foam structure have a major influence on the mechanical properties. The XPS foam has a relatively uniform morphology, whereas the morphology of EPS is characterized by a micro- and macro-porosity and commonly with randomly distributed voids between the beads. The origin of these pore-like defects is the partially incomplete contact of the foamed beads in the mould.

In Figure 4b the curves from the static compression tests at 23 °C for EPP with different densities and E-PBT are shown. The collapse stress of the EPP foams increase significantly with density. It can also be seen that the densification at a higher foam density is already achieved at a lower compression load. Both phenomena have

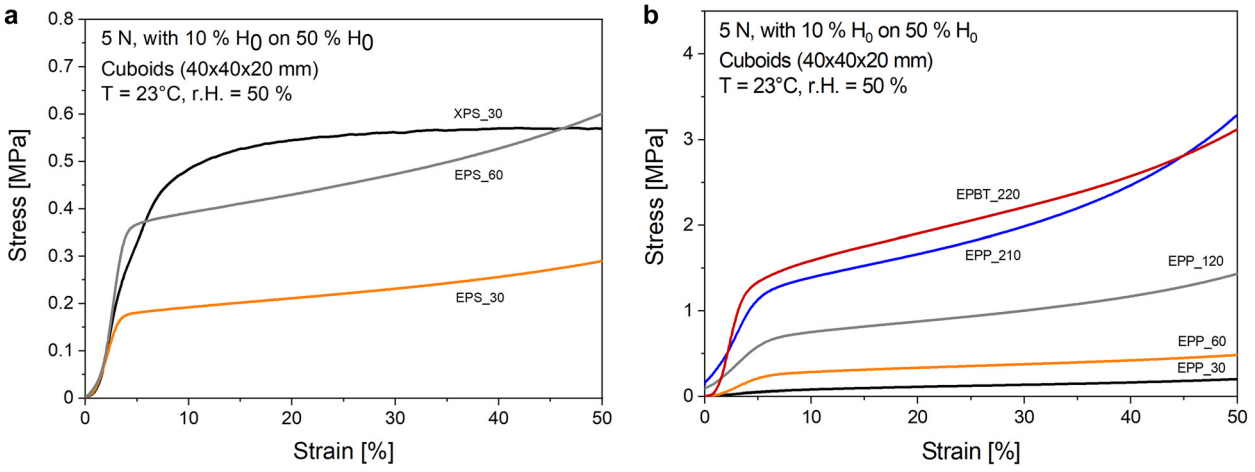

Figure 4: Static compression tests according to DIN EN ISO 844. (a) XPS_30, EPS_30, and EPS_60 and (b) EPP_30, EPP_60, EPP_120, EPP_210, and E-PBT_220. Please mind the different scales.

already been described in various publications [4, 6, 40]. All of the examined EPP foams show viscous behavior at a relative compression of 10%. The related compression stress for 10% deformation does not increase linearly with the relative foam density of the samples. For example, by increasing the density of EPP from 30 to 60 kg/m^3, the compression stress for 10% deformation increases by a factor of four. By further doubling of the foam density to 120 kg/m^3, the resulting compression stress roughly quintuples as well. All measured values are summarized in Table 2. The comparison of the compression behavior of EPP_210 and E-PBT_220 at 23 °C and 10% compression deformation shows that E-PBT has a slightly stronger resistance against deformation at the same density. This can be attributed to several aspects, among others the different cell morphology (e.g., possibly thicker cell struts of E-PBT) and differences in stiffness and ductility (e.g., a rather high ductility is known for PP [41])

Based on the compression stress necessary for 10% deformation ($\sigma_{10\%}$) which is determined at 23 °C with the static compression tests the corresponding test load $\sigma_{(10/10)\%}$ could be easily calculated. This stress is then applied as constant test load in the steady creep test with temperature steps (step 2). The most relevant data of the static compression tests and thermal investigation (DSC) is summarized in Table 2.

3.2.2 Step 2: steady creep test with stepwise increased temperature

Figure 5 shows the curves of the steady creep test with temperature steps for an extrusion foam and two bead foams of polystyrene; namely XPS_30, EPS_30, and EPS_60.

The relative compression of XPS_30, EPS_30, and EPS_60 is plotted against the temperature. The heating steps between 90 and 100 °C were reduced to 3 K in order to determine the T_{HS} more precisely. As can be seen from Figure 5, only a minor increase of the relative compression is visible for all foams tested up to a core temperature of 90 °C. An exponential increase in relative compression can be noted. Further, it can be seen that the measured values vary widely at 100 °C. Both indicate that the heat stability of the foams has been exceeded. Taking 10% relative compression as criteria, all examined amorphous foams (i.e., EPS and XPS) have a heat stability temperature of 98 °C even though from the supporting SEM images (cf. Figure 3) it is clearly visible, that the foam appearance including expansion, cell sizes micro- and macroporosity is different for the samples. From the measured values, it seems that neither the foam structure nor the density has a major influence on the T_{HS} of the investigated amorphous foams. However, the long measuring times due to the thermal inertia of the foams could be seen as disadvantageous. Though, this issue could be shortened by smaller measuring chambers and tools.

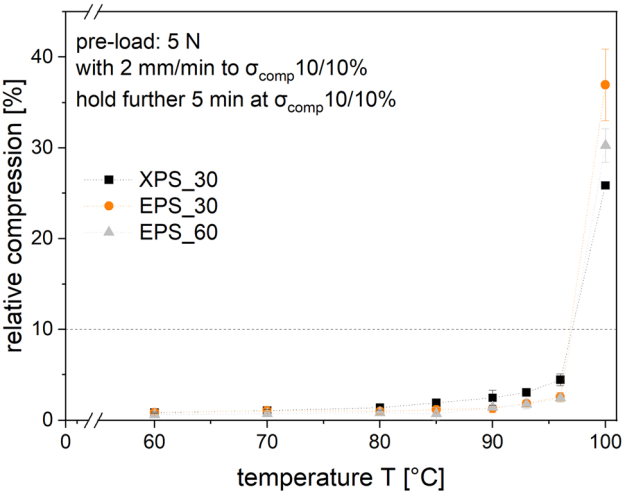

Figure 5: Steady creep test with temperature steps of XPS _30, EPS _30, and EPS_60.

Table 2: Important values of the DSC analysis and static compression test according to DIN EN ISO 844 (1st step).

Sample	DSC				Compression test DIN EN ISO 844			
	T_g (°C)	$T_{m,1}$ (°C)	$T_{m,2}$ (°C)	χ (%)	E_c (N/mm^2)	σ_{max} (MPa)	$\sigma_{10\%}$ (MPa)	$\sigma_{(10/10)\%}$ (MPa)
XPS_30	101	–	–	–	5.44	0.65	0.48	0.048
EPS_30	105	–	–	–	0.28	0.34	0.19	0.019
EPS_60	105	–	–	–	0.81	0.72	0.39	0.039
EPP_30	n/a	148	158	20.61/7.93[a]	0.66	0.26	0.08	0.008
EPP_60	n/a	155	164	23.97/0.91[a]	3.34	0.59	0.28	0.028
EPP_120	n/a	147	156	14.87/3.93[a]	11.59	1.71	0.75	0.075
EPP_210	n/a	151	159	20.93/3.63[a]	22.61	3.94	1.36	0.136
E-PBT_220	47	225	–	32.5	13.11	3.94	1.54	0.154

[a]EPP shows two melt peaks; values depict the crystallinity of first and second melting peak separately.

The approach of the steady creep test with temperature steps was furthermore applied to EPP samples with different densities of 30, 60, 120, and 210 kg/m^3, respectively. The results are shown in Figure 6a.

It can be seen clearly from Figure 6a that up to a limit of 80 °C, all curves have approximately a similar relative compression course regardless of the foam density. The curves diverge slightly depending on the foam density.

The change in mechanical properties under compression load can be attributed to the individual softening of the polymer. EPP_30, EPP_60 and EPP_120 achieved the test criterion, 10% relative compression based on the initial thickness, at around 100 °C. In contrast, EPP_210 achieved the test criterion at a slightly higher temperature of 107 °C. The deviation could be caused by different facts, such as (i) the usage of different PP grades with different thermal properties, (ii) unavoidable variations between the samples structure (e.g., voids) and (iii) the different appearance of the foam (density and cell morphology) – an aspect, whose influence has been reduced but not erased fully.

According to the concept of the chosen approach, by applying a rather low mechanical load related to the individual foam (morphology and density), the determined T_{HS} of the EPP foams should give approximately the same temperature. A plot of the measured T_{HS} against foam density should therefore ideally result in a horizontal line. The test criterion of 10% relative compression, selected according to DIN 53424, was plotted against the foam density in Figure 6b showing a slight slope of the trend line. In addition, the T_{HS} of the same foams was determined with a test criterion of 5 and 15% relative compression, in order to make a statement about the quality of the test criterion. Remarkable standard deviations for the 5% test criterion are visible, which is why it can be classified as insufficient. All T_{HS} values were furthermore summarized in Table 3.

Table 3: Values for the heat stability temperature T_{HS} obtained from the steady creep tests with temperature steps (2nd step) with different test criteria (5, 10 and 15% of relative compression).

Samples	Heat stability temperature (5% compr.) (°C)	Heat stability temperature (10% compr.) (°C)	Heat stability temperature (15% compr.) (°C)
XPS_30	97	98	99
EPS_30	97	98	98
EPS_60	97	98	99
EPP_30	75	101	107
EPP_60	85	102	108
EPP_120	70	99	106
EPP_210	60	107	113
E-PBT_220	169	186	193

The recommended test criterion of 10% relative compression is marked in orange.

For the test criteria 5 and 15% relative compression, the T_{HS} was determined in a range of 60–85 °C and 106–113 °C, respectively. The values at lower relative compression (i.e., 5%) scatter stronger which can be attributed to the different mechanical properties due to the formulations and different fusion conditions. In contrast, the spread of the measured temperatures decreases slightly with a compression of 15% (i.e., ΔT_{HS} = 7 K) compared to the specified test criterion of 10% compression i.e., ΔT_{HS} = 8 K). Here, the measured temperature increases slightly with the relative density, too. This reveals that the deviation of the obtained T_{HS} values is lower if a higher relative compression is selected as test criterion.

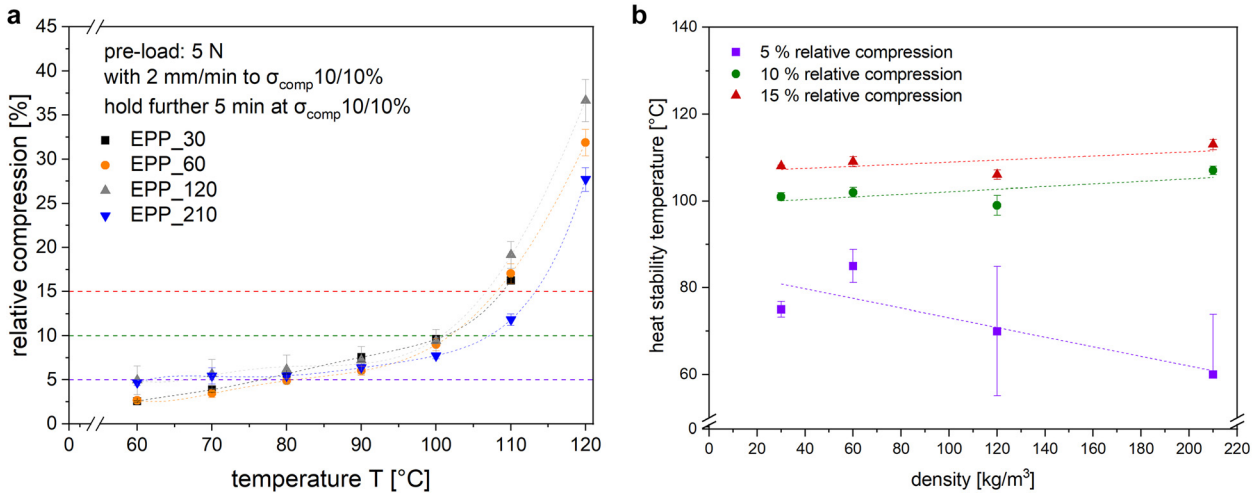

Figure 6: (a) Steady creep test with temperature steps of EPP with different densities. (b) Heat stability temperature versus foam density of EPP.

The comparison of the test criteria shows that the selected criterion of 10% relative compression can describe the material behavior of the selected EPP with an acceptable deviation of approx. 10%. Using the test criterion of 10% relative compression the deviation for T_{HS} was +/− 1 to 2 K for each of the investigated foams.

Furthermore, the comparison of Figures 5 and 6a clearly reveals that the material behavior of the semi-crystalline EPP foam significantly differs from that of the amorphous PS foam. For PS foams, there is an almost constant relative compression until the T_{HS} is reached closely to its T_g (cf. Figure 5). In contrast, for EPP up to a core temperature of 100 °C, a gradual increase in deformation behavior can be observed. For EPP which is examined above its T_g, a significantly higher tendency to creep can be assumed, which also increases with higher temperature, as the chain mobility correspondingly increases. Takemori et al. [31] found comparable material behaviors for compact amorphous and semi-crystalline thermoplastics with the help of DMA measurements.

Finally, the approach was applied to a novel bead foam made from the engineering polymer polybutylene terephthalate (E-PBT) as shown in Figure 7. From static compression tests at different temperatures up to 150 °C, it is known that the compression strength decreases with increasing temperature [30]. The resulting curve of the steady creep with temperature steps of E-PBT seems to be very similar to that of EPP foams but is located at elevated temperature. A T_{HS} of 186 °C was determined which is significantly higher than EPP_210 (107 °C).

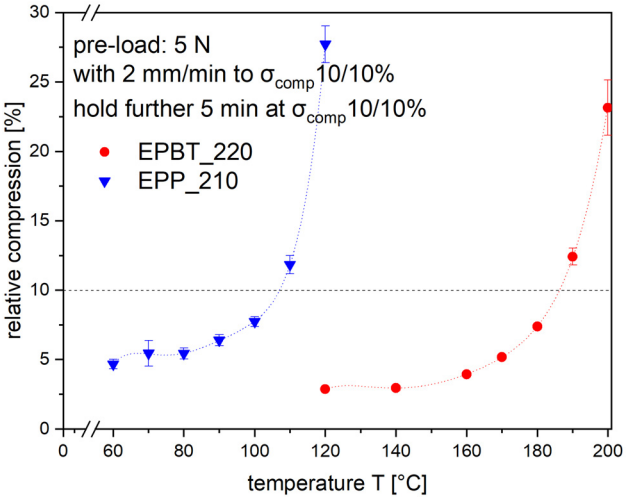

Figure 7: Steady creep tests with stepwise increased temperature of EPP_210 and E-PBT_220.

4 Conclusions

The principle of the chosen engineer-technical approach to use a low test load (stress), that would not lead to plastic deformation at room temperature enables the determination of a quantitative temperature value for the withstand of foams against a thermal load. We suggest calling the obtained value heat stability temperature T_{HS}. It can be concluded that this attempt allows to judge (and compare) foams with different densities and structures. The chosen approach is advantageous compared to other techniques:

(i) Unlike using a heating ramp, the procedure with stepwise increase of the temperature and holding periods for a certain time leads to an even temperature distribution within the foam bulk.

(ii) The low load, which is proportional to the compression strength of each material, minimizes its own impact on the deformation and maximizes the impact of thermal load.

For polystyrene foams (i.e., XPS and EPS), the T_{HS} determined was 98 °C. A range from 99-107 °C for polypropylene foams (i.e., EPP) and 186 °C for E-PBT was determined. The slight deviations in case of EPP are likely caused by the differences in the foam appearance (i.e., density and/or structure) and/or the fact that different grades with different thermal properties were investigated. However, the deviation is considered as acceptable. Though, the influence of the crystallinity on the T_{HS} is another fact that should be investigated in prospective works. Amorphous and semi-crystalline materials behave differently. Amorphous polystyrene shows a sudden change in compression behavior approaching its T_g, while the semi-crystalline polypropylene and polybutylene terephthalate followed a slower, but continuous change. Here, semi-crystalline polymers tend to creep as the measurements were carried out above their respective T_g.

In summary, the chosen approach suits excellently to analyze the behavior of polymeric foams under thermal load.

Acknowledgements: The authors would kindly like to thank (in alphabetic order) Alexander Brückner, Andreas Mainz and Annika Pfaffenberger for their technical support and meaningful advice as well as all the scientific staff members who contributed with inspiring discussions. Furthermore, Peter Schreier, Max Löhner and Tobias Dressendörfer from Neue Materialien Bayreuth GmbH are acknowledged for supplying and steam chest moulding EPS, EPP and E-PBT samples. The support of Bavarian Polymer Institute (BPI) is further acknowledged.

Author contributions: All the authors have accepted responsibility for the entire content of this submitted manuscript and approved submission.
Research funding: This study was funded by German Research Foundation DFG (AL 474/45-1), DFG (AL 474/51-1) and DFG (AL 474/42-1).
Conflict of interest statement: The authors declare that they have no conflicts of interest regarding this article.

References

1. Ashby M. F. The mechanical properties of cellular solids. *Metall. Trans. A* 1983, *14*, 1755–1769.
2. Ashby M. F. The properties of foams and lattices. *Philos. Trans. R Soc. A Math. Phys. Eng. Sci.* 2006, *364*, 15–30.
3. Avalle M., Belingardi G., Montanini R. Characterization of polymeric structural foams under compressive impact loading by means of energy-absorption diagram. *Int. J. Impact Eng.* 2001, *25*, 455–472.
4. Bouix R., Viot P., Lataillade J. L. Polypropylene foam behaviour under dynamic loadings: strain rate, density and microstructure effects. *Int. J. Impact Eng.* 2009, *36*, 329–342.
5. Mills N. J., Fitzgerald C., Gilchrist A., Verdejo R. Polymer foams for personal protection: cushions, shoes and helmets. *Compos. Sci. Technol.* 2003, *63*, 2389–2400.
6. Wei P., Liu L. Influence of density on compressive properties and energy absorption of foamed aluminum alloy. *J. Wuhan Univ. Technol. Mater. Sci. Ed.* 2007, *22*, 225–228.
7. Ramsteiner F., Fell N., Forster S. Testing the deformation behaviour of polymer foams. *Polym. Test.* 2001, *20*, 661–670.
8. Lim G. T., Altstädt V., Ramsteiner F. Understanding the compressive behavior of linear and cross-linked poly(vinyl chloride) foams. *J. Cell. Plast.* 2009, *45*, 419–439.
9. Standau T., Zhao C., Murillo Castellón S., Bonten C., Altstädt V. Chemical modification and foam processing of polylactide (PLA). *Polymers (Basel)* 2019, *11*, 306.
10. Winterling H., Sonntag N. *Polystyrol-Hartschaumstoff*; Kunststoffe, 2011.
11. Becker G. W., Braun D., Gausepohl H., Gellert R. *Kunststoff Handbuch Polystyrol Band 4*; Carl Hanser Verlag: Munich, 1995.
12. Tammaro D., Astarita A., Di Maio E., Iannace S. Polystyrene foaming at high pressure drop rates. *Ind. Eng. Chem. Res.* 2016, *55*, 5696–5701.
13. Tammaro D., Walker C., Lombardi L., Trommsdorff U. Effect of extrudate swell on extrusion foam of polyethylene terephthalate. *J. Cell. Plast.* 2020.
14. Gude M., Koschichow R., Liebsch A., Müller M., Stegelmann M. Morphological analysis and numerical modelling of the mechanical behaviour of polypropylene bead foams. In *7th International Conference on Mechanics and Materials in Design*, 2017; pp. 569–574.
15. Coquard R., Baillis D. Modeling of heat transfer in low-density EPS foams. *J. Heat Transf.* 2006, *128*, 538–549.
16. Ossa A., Romo M. Micro- and macro-mechanical study of compressive behavior of expanded polystyrene geofoam. *Geosynth. Int.* 2009, *16*, 327–338.
17. Standau T., Murillo Castellón S., Delavoie A., Bonten C., Altstädt V. Effects of chemical modifications on the rheological and the expansion behavior of polylactide (PLA) in foam extrusion. *E-Polymers* 2019.
18. Castiglioni A., Castellani L., Cuder G., Comba S. Relevant materials parameters in cushioning for EPS foams. *Colloids Surf. A Physicochem. Eng. Asp.* 2017, *534*, 71–77.
19. Di Landro L., Sala G., Olivieri D. Deformation mechanisms and energy absorption of polystyrene foams for protective helmets. *Polym. Test.* 2002, *21*, 217–228.
20. Dörr D., Raps D., Kirupanantham D., Holmes C., Altstädt V. *Expanded Polyamide 12 Bead Foams (ePA) Thermo-Mechanical Properties of Molded Parts*, 2020.
21. Strasser J. P. *Process for Producing PET Pellets, and PET Pellets, WO2011063806A1*, 2011.
22. Standau T., Hädelt B., Schreier P., Altstädt V. Development of a bead foam from an engineering polymer with addition of chain extender: expanded polybutylene terephthalate. *Ind. Eng. Chem. Res.* 2018, *57*, 17170–17176.
23. *DIN EN ISO 75-1 Bestimmung der Wärmeformbeständigkeitstemperatur*; Beuth Verlag: Berlin, Germany, 2013.
24. *DIN EN ISO 306 Bestimmung der Vicat-Erweichungstemperatur (VST)*; Beuth Verlag: Berlin, Germany, 2014.
25. *DIN 53424 Bestimmung der Formbeständigkeit in der Wärme bei Biegebeanspruchung und bei Druckbeanspruchung*; Beuth Verlag: Berlin, Germany, 1978.
26. Yeo S. S., Hsuan Y. G. Effects of temperature and stress on the short and long-term compressive behavior of expanded polystyrene. *Geosynth. Int.* 2009, *16*, 374–383.
27. Krundaeva A., De Bruyne G., Gagliardi F., Van Paepegem W. Dynamic compressive strength and crushing properties of expanded polystyrene foam for different strain rates and different temperatures. *Polym. Test.* 2016, *55*, 61–68.
28. Zhang J., Kikuchi N., Li V., Yee A., Nusholtz G. Constitutive modeling of polymeric foam material subjected to dynamic crash loading. *Int. J. Impact Eng.* 1998, *21*, 369–386.
29. Morton D. T., Reyes A., Clausen A. H., Hopperstad O. S. Mechanical response of low density expanded polypropylene foams in compression and tension at different loading rates and temperatures. *Mater. Today Commun.* 2020, *23*, 100917.
30. Standau T., Schreier P., Hilgert K., Altstädt V. *Properties of Bead Foams with Increased Heat Stability Made from the Engineering Polymer Polybutylene Terephthalate (E-PBT)*, 2020.
31. Takemori M. T. Towards an understanding of the heat distortion temperature of thermoplastics. *Polym. Eng. Sci.* 1979, *19*.
32. Hirai T., Nishijima K., Ochiai T. *Polylactic Acid Resin Foam Particle for In-Mold Foam Forming, Process for Producing the Same, and Process for Producing Polylactic Acid Resin Foam Molding, EP2135724A1*; European Patent Office: Munich, Germany, 2009.
33. Sampath B. D. S., Kriha O., Ruckdäschel H., Desbois P., Gruber F., Hahn K. *Expandable Pelletized Materials Based on Polyesters US 2012/0041086 A1*; United States Patent and Trademark Office: Alexandria, Virginia, USA, 2012.
34. Standau T., Nofar M., Dörr D., Ruckdäschel H., Altstädt V. A review on multifunctional epoxy-based Joncryl® ADR chain extended thermoplastics. *Polym. Rev.* 2021, *0*, 1–55.
35. Grein C., Plummer C. J. G., Kausch H. H., Germain Y., Béguelin P. Influence of β nucleation on the mechanical properties of isotactic polypropylene and rubber modified isotactic polypropylene. *Polymer (Guildf)* 2002, *43*, 3279–3293.

36. Illers K. H. Heat of fusion and specific volume of poly(ethylene terephthalate) and poly(butylene terephthalate. *Colloid Polym. Sci.* 1980, *258*, 117–124.
37. Gibson L. J., Ashby M. F. Thermal, electrical and acoustic properties of foams. *Cell Solids* 2014, 283–308.
38. Solórzano E., Rodriguez-Perez M. A., Lazaro J., De Saja J. A. Influence of solid phase conductivity and cellular structure on the heat transfer mechanisms of cellular materials: diverse case studies. *Adv. Eng. Mater.* 2009, *11*, 818–824.
39. Norton F. J. Thermal conductivity and life of polymer foams. *J. Cell. Plast.* 1967, *3*, 23–37.
40. Avella M., Bogoeva-Gaceva G., Bužarovska A., Errico M. E., Gentile G., Grozdanov A. Poly(lactic acid)-based biocomposites reinforced with kenaf fibers. *J. Appl. Polym. Sci.* 2008, *108*, 3542–3551.
41. Standau T., Pospiech D., Pötschke P., Kretzschmar B., Vogel R., Häußler L., Harre K., Koutsoumpis S., Pissis P., Logakis E. Preparation and properties of thermally conductive polypropylene composites. *Z. Kunststofftechnik / J. Plast. Techn.* 2016, *12*, 465–496.